THE ASTRONOMICAL JOURNAL VOLUME 114, NUMBER 3 SEPTEMBER 1997

PHYSICAL MODEL OF NEAR-EARTH ASTEROID 6489 GOLEVKA (1991 JX) FROM OPTICAL AND INFRARED OBSERVATIONS[1]

S. MOTTOLA, A. ERIKSON, A. W. HARRIS, G. HAHN, AND G. NEUKUM

DLR, Institute of Planetary Exploration, D-12489 Berlin, Germany
Electronic mail: Stefano.Mottola, Anders.Erikson, Alan.Harris, Gerhard.Hahn, Gerhard.Neukum@dlr.de

M. W. BUIE

Lowell Observatory, Flagstaff, Arizona 86001
Electronic mail: buie@lowell.edu

W. D. SEARS[2] AND A. W. HARRIS

Jet Propulsion Laboratory, Pasadena, California 91109
Electronic mail: wsears@stsci.edu, awharris@lithos.jpl.nasa.gov

D. J. THOLEN AND R. J. WHITELEY

Institute for Astronomy, 2680 Woodlawn Drive, Honolulu, Hawaii 96822
Electronic mail: tholen@galileo.ifa.hawaii.edu, robw@ifa.hawaii.edu

P. MAGNUSSON AND J. PIIRONEN[3]

Astronomiska Observatoriet, Box 515, S-75220 Uppsala, Sweden
Electronic mail: Per.Magnusson@astro.uu.se, jpiirone@gstar.astro.helsinki.fi

T. KWIATKOWSKI AND W. BORCZYK

Astronomical Observatory of Adam Mickiewicz University, 60-286 Poznan, Poland
Electronic mail: tkastr@phys.amu.edu.pl

E. S. HOWELL,[4] M. D. HICKS, AND R. FEVIG

Lunar and Planetary Laboratory, Tucson, Arizona 85721
Electronic mail: ehowell@qualibou.upr.clu.edu, hicksm@lpl.arizona.edu, fevig@plains.nodak.edu

YU. N. KRUGLY, F. P. VELICHKO, AND V. G. CHIORNY

Astronomical Observatory of Kharkiv State University, 31022 Kharkiv, Ukraine
Electronic mail: krugly@astrom.kharkov.ua, velichko@astrom.kharkov.ua, chiorny@astrom.kharkov.ua

N. M. GAFTONYUK

Astronomical Observatory, 334242 Simeis, Ukraine

M. DI MARTINO

Osservatorio Astronomico di Torino, I-10025 Pino Torinese, Italy
Electronic mail: dimartino@to.astro.it

P. PRAVEC

Astronomical Institute, Czech Academy of Sciences, CZ-25165 Ondrejov, Czech Republic
Electronic mail: ppravec@asu.cas.cz

L. ŠAROUNOVÁ AND M. WOLF

Astronomical Institute, Charles University, CZ 15000 Prague, Czech Republic
Electronic mail: lenka@asu.cas.cz

W. WORMAN

Department of Physics and Astronomy, Moorhead State University, Moorhead, Minnesota 56563
Electronic mail: worman@mhdha.moorhead.msus.edu

J. K. DAVIES

Joint Astronomy Centre, Hilo, Hawaii 96720
Electronic mail: jkd@jach.hawaii.edu

 0004-6256/97/114(3)/1234/12/$10.00

H.-J. SCHOBER
Institut für Astronomie, A-8010 Graz, Austria
Electronic mail: schober@bkfug.kfunigraz.ac.at

W. PYCH
Warsaw University Astronomical Observatory, 00-478 Warsaw, Poland
Electronic mail: pych@sirius.astromw.edu.pl

Received 1997 February 10; revised 1997 May 27

ABSTRACT

In 1995 asteroid 6489 Golevka (1991 JX) had a close encounter with the Earth at a distance of 0.034 AU, providing a good opportunity for a detailed study of a small Solar System object. In this paper we report the results of an extensive international observing campaign aimed at determining Golevka's rotational and physical properties from optical photometry and thermal IR radiometry. From the analysis of photometric light curves we derive a spin axis model whose coordinates are λ_p (J2000)=347°±10° and β_p (J2000)=35°±10°. The strict periodicity observed in light curves taken during virtually constant illumination and observing conditions argues against free precession of the spin vector. The rotation is prograde with a sidereal period P_{sid}=0.25110±0.00001 d (6.02640±0.00024 hr). The derived ellipsoidal shape model results in a/b=1.4±0.2, while not satisfactorily constraining the b/c ratio. No systematic V–R color index variation larger than 0.005 mag (1σ) was observed, suggesting a spectrally uniform surface on a hemispheric scale. The integral phase curve is moderately well represented by the H-G parameter system that fails, however, to reproduce the observed opposition spike. We derive mean H, G values of 19.074 ±0.029 and 0.138±0.013, respectively. The application of the more accurate Hapke photometric function produces a better fit and allows us to describe the surface scattering properties in terms of model parameters: $\bar{\vartheta}$=7°±7°, g=−0.435±0.001, $\bar{\omega}_0$=0.58±0.03, h=0.0114±0.0004, B_0=0.758±0.014. Infrared measurements reveal that the flux at 10.6 μm is unusually small in view of the object's optical brightness. The combined application of a modified Fast Rotating Thermal Model and of the photometric model suggests that Golevka is a small body with approximate dimensions (0.35×0.25×0.25 km) and a very high geometric albedo p_v~0.6. However, the possible effect of model assumptions on these latter results still has to be explored. © *1997 American Astronomical Society.* [S0004-6256(97)01809-8]

1. INTRODUCTION

Near-Earth Objects (NEOs) represent one of the most interesting classes of bodies in the Solar System. From a scientific point of view they allow insights into the physical and dynamical processes that shaped the asteroid belt: accretion into planetesimals, collisions, and gravitational perturbations by the giant planets. Currently (1997 January) some 400 NEOs are known, less than half of which have reliable orbital determinations.

The Apollo-type object (see Shoemaker *et al.* 1979, for a definition of the orbital classes) 6489 Golevka (1991 JX) was discovered by E.F. Helin with the 0.46 m Schmidt telescope at Palomar on 1991 May 10 (Helin 1991) a few weeks before it approached the Earth to within 0.033 AU. Subsequent optical and radar (Ostro *et al.* 1991) observations allowed an accurate determination of its orbital parameters (Williams 1995), and showed that this sub-km sized object is orbiting close to the 3:1 mean-motion resonance with Jupiter. Orbital integrations performed by one of us (G. H.) for the period from 1900 to 2100, show the strong influence of the 3:1 jovian resonance on the osculating orbit of 6489 Golevka.

From these computations it appeared that, apart from the discovery apparition in 1991, Golevka's closest approach to the Earth during the integration period was in 1995 (see Fig. 1), which offered particularly favorable observing conditions. We therefore decided to organize an observing campaign to follow the asteroid over a wide range of viewing conditions, which would enable rotational parameters of 6489 Golevka to be derived from one single apparition. Additional motivation was also provided by the international radar campaign (Ostro *et al.* 1995a), planned for the time of closest approach in 1995 June, which would allow a comprehensive study of the physical parameters of this object. This approach has already been successfully applied during the close encounters of 4179 Toutatis in 1992–1993 (Spencer *et al.* 1995; Ostro *et al.* 1995b) and 1620 Geographos in 1994 (Magnusson *et al.* 1996; Ostro *et al.* 1996).

2. OBSERVATIONS

To determine a reliable spin vector solution and a shape model for an asteroid, it is important to have observations

[1]This work is partly based on observations collected at the European Southern Observatory.
[2]Presently with Computer Sciences Corporation at STScI, Baltimore.
[3]On leave from Observatory, University of Helsinki, Finland.
[4]Currently at University of Puerto Rico, Mayaguez.

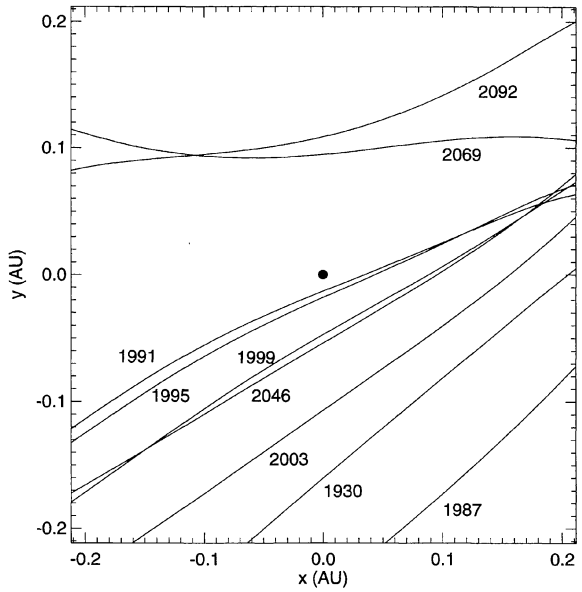

FIG. 1. Projection onto the ecliptic plane of the orbit of 6489 Golevka expressed in a geocentric reference system over the integration period 1900–2100.

spread over a wide range of ecliptic longitudes. While this strategy requires observations to be made over several apparitions for a typical main-belt object, it often happens that during a NEO close approach the viewing geometry spans a sufficiently broad range in just one apparition. The 1995 apparition of Golevka provided such an opportunity. However, a complication with a NEO close approach is the large and simultaneous changes of aspect and solar phase angle, which have to be disentangled in the analysis.

The observations of 6489 Golevka reported in this paper were carried out during the 1995 apparition from 11 observing stations in 6 different countries. To learn as much as possible about this object during this favorable encounter, close cooperation of the observers and careful planning were necessary. As a result, uniform sampling during the whole apparition was possible and unnecessary repetitions could be avoided.

The first observations started in early 1995 April from the southern hemisphere as soon as the asteroid became brighter than the limiting magnitude of our instrumentation. From the first light curve it was immediately evident that the rotation period was almost exactly 6 hours, and the prompt communication of this result enabled other observers to plan their observations accordingly. This procedure also allowed us to organize continuous observations from stations located at different longitudes, and helped us resolve a possible aliasing in the determination of Golevka's period due to its commensurability with the Earth rotation.

During the same month the solar phase angle decreased rapidly, to reach its minimum value around April 23. In fact, during the observations made on the same day from Ondrejov, the Earth as seen from Golevka appeared in transit across the disk of the Sun. However, the angular diameter of the Earth as seen from the asteroid was about 24 times smaller than that of the Sun, therefore producing a reduction of the solar flux of about 0.002 mag, too small to affect our data to any measurable degree.

Measurements were performed throughout the asteroid's close encounter with the Earth with the exception of a 43-day period when the solar elongation was too small to enable us to obtain meaningful results, and continued through the end of August when Golevka faded out again.

The observational circumstances and aspect data for each night of observation are summarized in Table 1. The table gives the heliocentric and geocentric distances, the solar phase angle, the object's geocentric ecliptic coordinates, the observatory and observers. The date of observation refers to the approximate mid-time of the observed lightcurve.

The observations were performed mostly with CCD photometers and in the Johnson V and R bands. In one case it was also possible to perform infrared thermal measurements at 10.6 μm. Due to the large number of researchers involved in this project, data reduction was performed using different techniques, which followed, however, the general guidelines given in Harris & Lupishko (1989).

The observations have resulted in over 50 single-night lightcurves. This bulk of data is archived in the Asteroid Photometric Catalogue maintained at Uppsala (Lagerkvist *et al.* 1987, and successive updates), and is available on the World Wide Web at the address http://www.astro.uu.se/planet/apc.html.

Selected composites obtained from light curves spanning the whole encounter sequence are shown in Fig. 2, and displayed with a rotation period P=6.026 hr. The magnitudes displayed in the graph are reduced to unit distance from the Earth and Sun, and the times are light-travel corrected. No correction for solar phase angle has in general been made. Only the light curve of April 23.2 [Fig. 2(b)], which was obtained at a very low phase angle and showed a large phase-induced magnitude variation within a single night, has been corrected with a linear phase coefficient, and referred to the phase of mid-observation, for plotting purposes only.

The curves are asymmetric and show considerable changes as the illumination and viewing geometry change, indicating a departure from a simple, ellipsoid-like shape. The lightcurve amplitude amounted to 0.37 mag during early April, and decreased to 0.28 mag in late April when the asteroid was exactly in opposition. With increasing solar phase angle and changing viewing geometry the amplitude increased again to reach its maximum value of 1.05 mag on June 6.2. In the meanwhile the asteroid was rapidly approaching the Earth, and on June 8, when it reached its minimum geocentric distance of 0.034 AU, it was moving with an apparent velocity of over 15° per day. By this time the solar elongation became small and this geometry allowed only short observations. On June 16, when the asteroid was close to its maximum brightness, it was possible to obtain infrared measurements in the 10.6 μm band. By late July the solar elongation increased again and it was possible to resume the photometric observations through the end of August, when Golevka had faded to V=18.7.

A striking feature in the lightcurves is the progressive dimming of what, during the pre-close approach observa-

TABLE 1. Observational circumstances.

Date	r (AU)	Δ(AU)	Phase angle (deg)	Ecl. Long (deg 2000)	Ecl. Lat. (deg 2000)	Observatory	Observer
1995 Apr 4.2	1.4324	0.4480	12.6	212.2	−1.7	ESO, La Silla	Mottola
1995 Apr 22.0	1.2954	0.2903	0.6	212.3	−0.2	Ondrejov Obs.	Pravec, Wolf, Šarounová
1995 Apr 22.3	1.2932	0.2880	0.4	212.2	−0.2	Table Mountain Obs.	Sears, Harris (JPL)
1995 Apr 23.0	1.2880	0.2827	0.1	212.2	−0.1	Ondrejov Obs.	Pravec, Wolf, Šarounová
1995 Apr 23.2	1.2866	0.2811	0.3	212.2	−0.1	ESO, La Silla	Erikson
1995 Apr 23.3	1.2858	0.2804	0.4	212.2	−0.1	Table Mountain Obs.	Sears, Harris (JPL)
1995 Apr 24.2	1.2793	0.2736	1.1	212.2	0.1	ESO, La Silla	Erikson
1995 Apr 24.3	1.2785	0.2729	1.2	212.2	0.1	Table Mountain Obs.	Sears, Harris (JPL)
1995 Apr 25.2	1.2720	0.2662	1.9	212.1	0.2	ESO, La Silla	Erikson
1995 Apr 25.3	1.2713	0.2655	2.0	212.1	0.2	Table Mountain Obs.	Sears, Harris (JPL)
1995 Apr 26.2	1.2648	0.2589	2.8	212.1	0.4	ESO, La Silla	Erikson
1995 Apr 27.9	1.2527	0.2469	4.2	212.0	0.7	Kharkiv Obs.	Velichko, Chiorny
1995 Apr 29.2	1.2434	0.2377	5.3	212.0	0.9	ESO, La Silla	Erikson
1995 May 2.2	1.2226	0.2173	7.9	211.9	1.5	ESO, La Silla	Erikson
1995 May 4.2	1.2090	0.2043	9.7	211.8	2.0	ESO, La Silla	Erikson
1995 May 7.2	1.1892	0.1853	12.5	211.8	2.8	ESO, La Silla	Erikson
1995 May 8.2	1.1827	0.1792	13.4	211.8	3.2	ESO, La Silla	Erikson
1995 May 19.2	1.1173	0.1164	23.5	213.0	8.5	Lowell Obs.	Buie
1995 May 21.2	1.1066	0.1058	25.4	213.6	10.0	Lowell Obs.	Buie
1995 May 22.8	1.0984	0.0975	26.8	214.2	11.5	Ostrowik Obs.	Kwiatkowski, Borczyk
1995 May 23.2	1.0964	0.0954	27.2	214.3	11.9	Lowell Obs.	Buie
1995 May 23.8	1.0936	0.0924	27.7	214.7	12.6	Ostrowik Obs.	Kwiatkowski, Borczyk
1995 May 26.3	1.0816	0.0800	30.0	216.2	15.7	Table Mountain Obs.	Sears, Harris (JPL)
1995 May 27.2	1.0775	0.0757	30.8	216.9	17.1	Table Mountain Obs.	Sears, Harris (JPL)
1995 May 27.9	1.0744	0.0723	31.4	217.5	18.2	Kharkiv Obs.	Velichko, Chiorny
1995 May 28.2	1.0731	0.0709	31.7	217.8	18.7	ESO, La Silla	Piironen
1995 May 28.3	1.0726	0.0705	31.8	217.9	18.9	Table Mountain Obs.	Sears, Harris (JPL)
1995 May 29.1	1.0692	0.0668	32.6	218.8	20.5	ESO, La Silla	Piironen
1995 May 29.3	1.0683	0.0659	32.8	219.0	20.9	Table Mountain Obs.	Sears, Harris (JPL)
1995 May 30.3	1.0642	0.0614	33.8	220.4	23.1	Table Mountain Obs.	Sears, Harris (JPL)
1995 May 31.2	1.0606	0.0575	34.9	221.8	25.3	ESO, La Silla	Piironen
1995 May 31.2	1.0606	0.0575	34.9	221.8	25.3	Paul Feder Obs.	Worman, Fevig
1995 Jun 1.2	1.0567	0.0534	36.1	223.8	28.1	Paul Feder Obs.	Worman, Fevig
1995 Jun 1.3	1.0563	0.0530	36.3	224.0	28.4	Table Mountain Obs.	Sears, Harris (JPL)
1995 Jun 3.2	1.0493	0.0458	39.5	229.3	35.1	Lowell Obs.	Buie
1995 Jun 4.9	1.0435	0.0404	43.6	236.9	42.5	Simeis Obs.	Krugly, Gaftonyuk
1995 Jun 5.2	1.0425	0.0396	44.5	238.5	43.9	Lowell Obs.	Buie
1995 Jun 6.2	1.0393	0.0372	47.9	245.5	48.8	Lowell Obs.	Buie
1995 Jun 7.0	1.0372	0.0360	51.2	255.3	53.0	Torino Obs.	Di Martino
1995 Jun 7.9	1.0343	0.0346	55.3	263.9	56.6	Simeis Obs.	Krugly, Gaftonyuk
1995 Jun 8.4	1.0329	0.0343	57.8	270.9	58.3	Catalina Obs.	Howell
1995 Jun 11.5	1.0251	0.0363	73.5	321.7	58.1	Mauna Kea Obs.	Tholen, Whiteley
1995 Jun 11.9	1.0242	0.0370	75.3	326.9	56.8	Simeis Obs.	Krugly, Gaftonyuk
1995 Jun 12.5	1.0229	0.0383	77.8	333.3	54.7	Mauna Kea Obs.	Tholen, Whiteley
1995 Jun 13.5	1.0209	0.0409	81.4	342.0	50.9	Mauna Kea Obs.	Tholen, Whiteley
1995 Jun 16.6	1.0157	0.0514	88.8	357.2	40.2	UKIRT, Mauna Kea	Davies
1995 Jul 28.3	1.1005	0.2285	62.5	18.6	10.8	ESO, La Silla	Erikson
1995 Jul 29.3	1.1056	0.2321	61.5	18.5	10.6	Table Mountain Obs.	Sears, Harris (JPL)
1995 Jul 30.4	1.1114	0.2361	60.3	18.5	10.5	Table Mountain Obs.	Sears, Harris (JPL)
1995 Jul 31.4	1.1168	0.2397	59.2	18.4	10.3	Table Mountain Obs.	Sears, Harris (JPL)
1995 Aug 1.4	1.1222	0.2433	58.1	18.3	10.1	Table Mountain Obs.	Sears, Harris (JPL)
1995 Aug 25.3	1.2778	0.3296	31.3	12.3	7.0	ESO, La Silla	Mottola, Schober
1995 Aug 31.3	1.3223	0.3558	24.5	9.9	6.2	ESO, La Silla	Mottola, Schober

tions, was the primary maximum, until its complete disappearance in the lightcurve of June 11. The disappearance of a light curve extremum, indicative of an irregular shape, has already been observed in other asteroids, but is very rarely observed in high-amplitude lightcurves.

The observations were also designed to search for possible non-periodic behavior in the lightcurves, which could be a sign of non-principal axis rotational motion. In particular, whenever possible, light curves were acquired during consecutive nights, and spanning the longest possible time interval within each individual night. The analysis of high accuracy measurements taken when the asteroid was still far from the Earth, with viewing and illumination geometry not changing appreciably during a few consecutive nights has

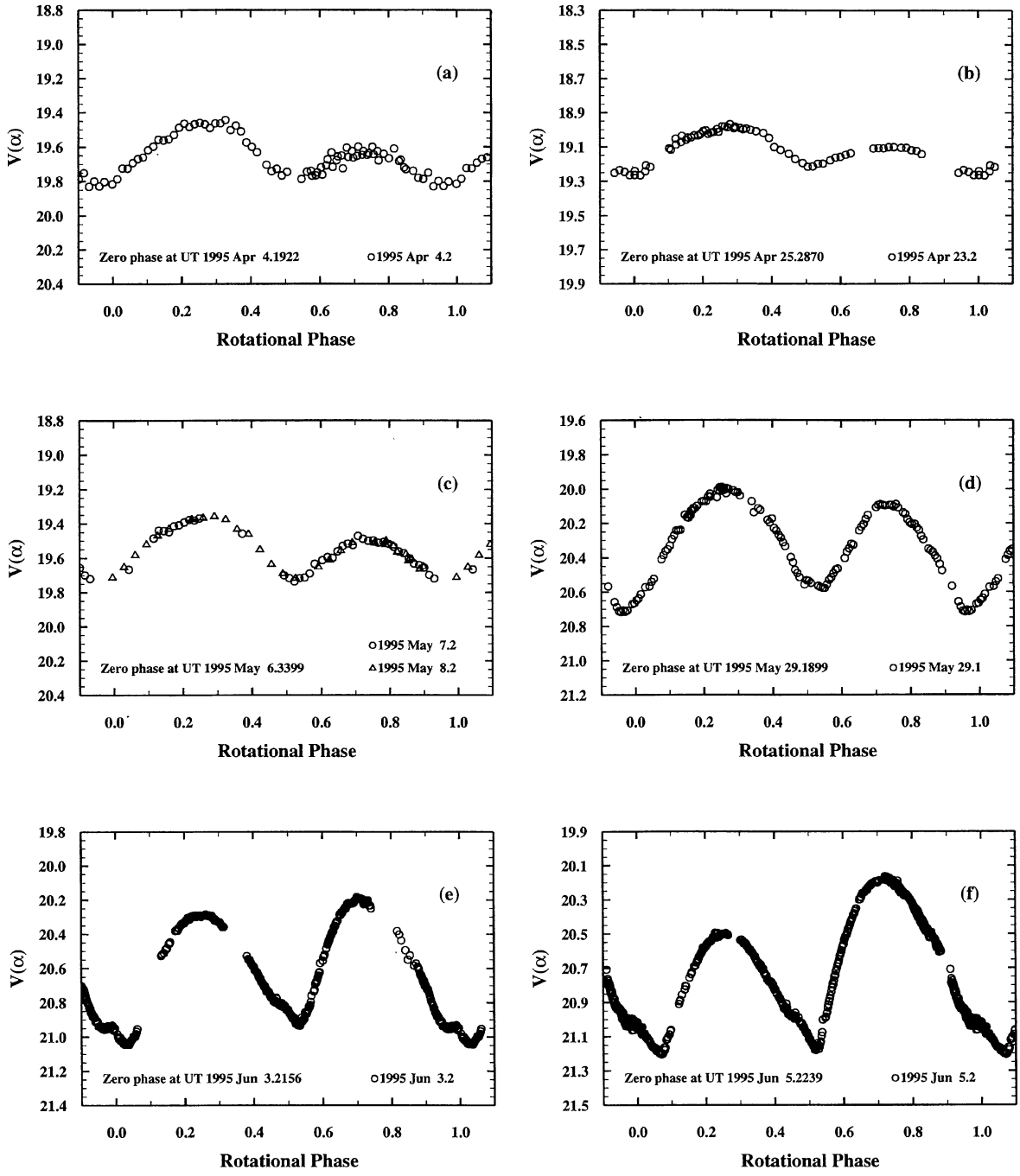

FIG. 2. Selected composites obtained from light curves of 6489 Golevka during the 1995 apparition. The rotation period used in the composites is $P=6.026$ hr. The sequence illustrates the dramatic change in the lightcurve shape during this period.

revealed a remarkably constant lightcurve shape, and we fail to detect any departure from a damped, principal-axis rotation state.

3. COLOR VARIATIONS

During the observations of May 8.2 time-resolved *V-R* color index measurements were obtained. The observations were performed by alternating exposures in the two filters and covering one full rotational cycle. The lightcurve amplitude in the *V* band at the time of the observation was 0.40 mag, the phase angle 13.4°, and the sub-Earth latitude 32.7°. Since the measurements in the two filters, although very close in time, were not acquired strictly simultaneously, we have interpolated the lightcurve in the *R* band with a high-

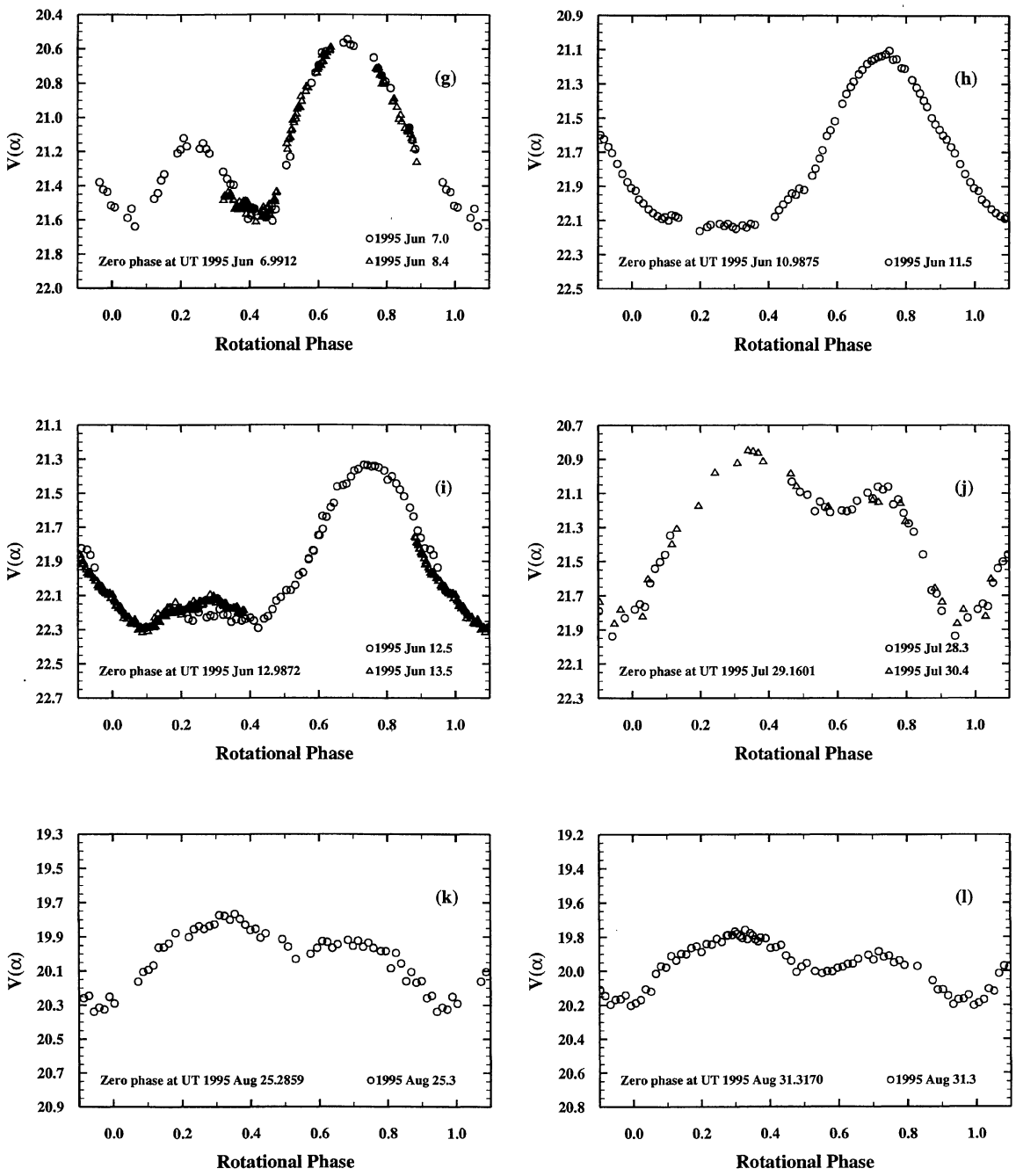

FIG. 2. (continued)

order Fourier polynomial, and subtracted this from each individual point in the other spectral channel. This procedure assures that no light-curve-induced color shifts are detected as spurious effects in the color lightcurves. The resulting color-index light curve is shown in Fig. 3. From these data no systematic rotational color variations larger than 0.005 mag (1σ) are evident, suggesting that the asteroid surface is characterized by a high degree of spectral uniformity on a hemispheric scale. The rotationally-averaged *V-R* color index is 0.454 ± 0.020.

Hicks & Grundy (1995) obtained a reflectance spectrum of Golevka in the range 0.55–1.05 μm, and found that it resembles that of Vesta. Our color determination is compatible with a *V*-type membership for Golevka; however, the *V-R* color index is not sufficiently diagnostic to confirm this classification.

4. SPIN VECTOR AND SHAPE MODELS

We present here two independent analyses using two different methods. Both techniques combine epochs (*E*) and

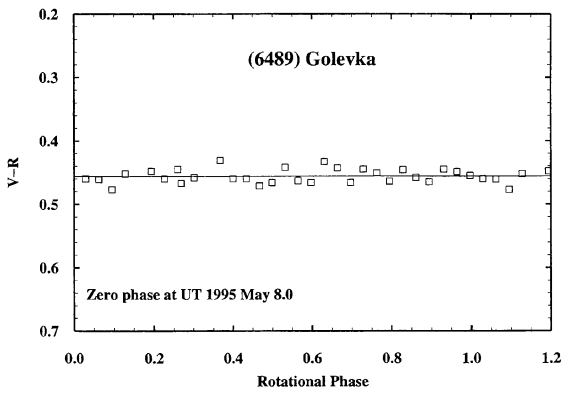

FIG. 3. Time-resolved *V-R* color-index measurements composited with a rotation period $P=6.026$ hr. No systematic color variations larger than 0.005 mag are detected.

lightcurve amplitude (A) information (see Magnusson *et al.* 1996 for a description) but differ in parametrization, least-squares fitting procedure, light scattering laws, and implementation used. Both methods approximate the photometric behavior of the asteroid as a triaxial ellipsoid having axes $a>b>c$ and rotating about the c axis. Although not always realistic for small, irregular objects, this approximation has been shown to produce good results even in cases where the actual shape of the object differed substantially from the assumed one (Magnusson *et al.* 1996). Solutions are expressed in terms of sidereal period, sense of rotation, coordinates of the spin axis and axial ratios (a/b, b/c) of the model ellipsoid (and orientation of the asteroid at a given time).

A complication that arises when using amplitude methods in the case of NEO close approaches, is the fact that it is necessary to disentangle the contributions of changing phase and aspect angle, since both quantities contribute to the lightcurve amplitude. The two different methods applied in this paper have different approaches to solve these difficulties, and comparison of the respective results gives information about the accuracy and consistency of the derived models.

4.1 Model I

This model, computed by P. Magnusson, is based on the method described in Magnusson (1986, 1990) and Erikson & Magnusson (1993). Amplitudes and epochs are determined by expanding the individual lightcurves to a low-order Fourier series and extracting the second order harmonic. In this way no difference between the amplitudes of primary and secondary extrema is considered in the model. Phase angle variations are accounted for by assuming a linear amplitude-phase relationship (see Sec. 4), as proposed in Zappalà *et al.* (1990). The phase correction coefficient is then determined simultaneously to the shape parameters in the least squares minimization routine. Because the linear approximation becomes inaccurate for large phase angles, the observations obtained between June 11 and June 14 have not been included in this analysis.

From this model, two spin vector solutions are obtained, one characterized by a prograde sense of rotation, the other by a retrograde one. The two solutions differ also in the value of the sidereal period of rotation, and this fact produces a half-cycle phase difference between the two solutions during the June/July gap in the observations. The model does not put firm constraints on the b/c ratio, which is then regarded as undetermined. The model solutions are summarized in Table 2. A formal error estimation gives unreasonably small errors, since the restriction to a single apparition with simultaneous changes of aspect and solar phase, coupled with a strongly irregular shape, could produce systematic effects in the results. Therefore, the tabulated errors are obtained using various subsets of the data, and using different methods for taking both the illumination and viewing geometries into account.

4.2 Model II

This model, computed by T. Kwiatkowski, uses the Simultaneous Epoch-Amplitude Method described in Kwiatkowski (1995). Input data consist of the lightcurve amplitudes, and of the epochs of the maxima. Model amplitudes are obtained by integrating Lommel-Seeliger's law over the surface of a triaxial ellipsoid, and computed for the same viewing and illumination geometry as the real observations. This procedure makes it unnecessary to reduce the observed amplitudes to a reference solar phase angle (generally 0°), thus reducing systematic errors when light curves obtained at large phase angles are used.

The physical model is based on six parameters: λ_p, β_p, a/b, b/c, $P_{\rm sid}$, and L_0 which represent the ecliptic longitude and latitude of the spin axis, the axial ratios of the ellipsoid shape, the sidereal period of rotation and the rotational phase at zero epoch, respectively. Residuals in amplitudes and epochs are minimized by allowing these parameters to vary iteratively.

As a first step, the whole celestial sphere is scanned by varying λ_p, β_p on a grid of 10°, and at each grid-point the

TABLE 2. Model solution summary.

Model	$P_{\rm sid}$(days)	Rotation sense	λ_p (J2000)	β_p (J2000)	a/b	b/c	Comments
I	0.25109±0.00001	Prograde	345°±10°	45°±10°	1.25±0.05		
I	0.25123±0.00001	Retrograde	190°±20°	−55°±10°	1.25±0.05		albedo variations required
II	0.25111±0.00002	Prograde	350°±10°	25°±10°	1.6±0.3	0.7±0.2	
II	0.25125±0.00001	Retrograde	200°±10°	−55°±10°	1.6±0.3	1.2±0.2	albedo variations required
adopted	0.25110±0.00001	Prograde	347°±10°	35°±10°	1.4±0.2	1.0	

remaining four parameters (a/b, b/c, P_{sid}, and L_0) are adjusted to obtain the best fit. This grid search detects three local minima, whose approximate coordinates are: S_1 ($\lambda_p = 200°$, $\beta_p = -65°$), S_2 ($\lambda_p = 350°$, $\beta_p = 25°$) and S_3 ($\lambda_p = 340°$, $\beta_p = -65°$). The third solution, however, yields an unrealistic, extremely flattened shape, and is therefore rejected.

The preliminary solutions S_1 and S_2 are then used as initial conditions for performing the final step, in which an iteration in the whole six dimensional parameter space is performed.

To better estimate systematic errors, connected with the non-ellipsoidal shape of the asteroid and the unknown scattering properties of its surface, calculations were performed with the maximum, average, and minimum amplitudes as well as with Lommel-Seeliger's and Hapke's scattering laws. Hapke's law was used with parameters typical for average C and S type asteroids (Helfenstein & Veverka 1989). As intuitively expected, the derived pole and periods were generally independent of the type of scattering law, with only the shape parameters being affected. The use of maximum, average, and minimum amplitudes, however, turned out to have a strong influence on the model, and the results presented in Table 2 were obtained by averaging the three corresponding solutions.

The uncertainties given there for each parameter are maximum errors rather than standard deviations. This choice reflects the fact that the statistical noise in the input data is smaller than the various systematic effects (Kwiatkowski 1995).

As in model I, we find one prograde and one retrograde solution, where the latter implies substantial albedo variations across the surface.

It might be worth noting that in the case of prograde rotation this model produces an unphysical value for the b/c ratio, which, by definition, should be equal to or larger than 1. This discrepancy serves as a reminder that the shape derived by these models corresponds to a "photometric" ellipsoid, that is the ellipsoid that best matches the photometric behavior of the body, and will in general differ from the actual shape of the body.

4.3 Adopted Model

Both models presented in this section converge on two pole solutions—a prograde one and a retrograde one. A comparison of the quality of fit of the two solutions gives no reason to reject either of them. However, the analysis of the lightcurves from April 4 and August 31 can give us additional information. The two lightcurves have very similar shapes, and were obtained when the asteroid was viewed from approximately opposite directions. One lightcurve was observed when the sub-Earth point was on the northern hemisphere of 6489 Golevka, and the other when it was on the southern hemisphere. For prograde rotation, qualitatively similar light variations are observed when the asteroid is observed from diametrically opposite directions (Fig. 4), which is consistent with such variations being produced by shape alone. By contrast, in order to explain the difference in the light scattered in diametrically opposite directions in the case

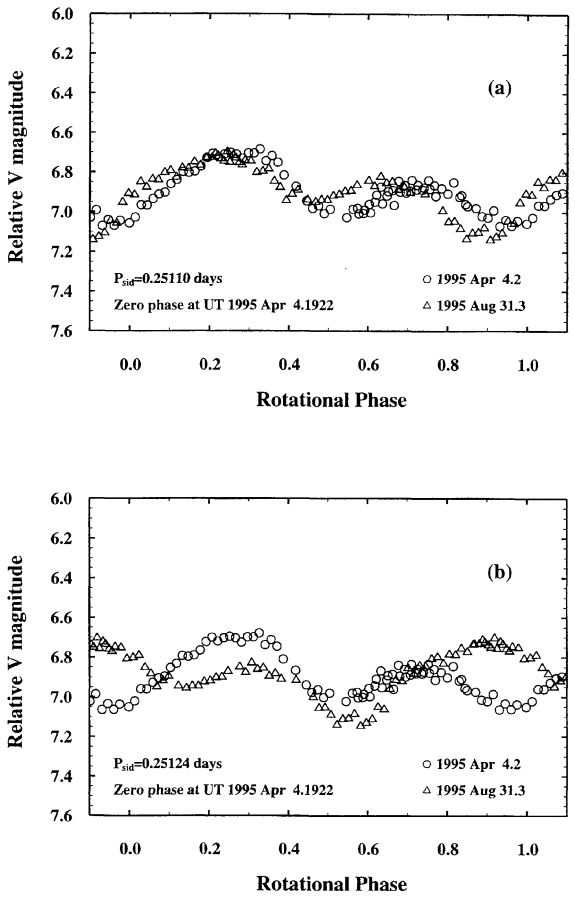

FIG. 4. Composite lightcurves obtained from the observations of 1995 April 4.2, and 1995 August 31.3, and using (a) the prograde solution and (b) the retrograde one.

of retrograde rotation, we have to postulate hemispheric-scale albedo differences exceeding the 10% level.

Based on our current knowledge about the nature of asteroids, it appears unlikely that Golevka's surface displays large, hemispheric-scale albedo variations. This view is also supported by the lack of rotationally-induced color variations in the V and R spectral bands (see Sec. 3). Therefore we favor the prograde rotation model, in which shape alone is responsible for asymmetries in the lightcurves, even though the possibility of retrograde rotation cannot be completely ruled out. The prograde rotation is confirmed by a preliminary analysis of the delay-Doppler imaging experiments reported in Hudson & Ostro (1995).

Both prograde models are in good agreement in terms of longitude of the pole, while they differ by 20° in latitude. The adopted solution is therefore derived from the average of the individual coordinates from the two models. As for the b/c ratio, none of the models can provide a satisfactory estimation, and for the purpose of further analysis we will assume that Golevka is best approximated by a biaxial ellipsoid ($a/b = 1.4$; $b/c = 1$).

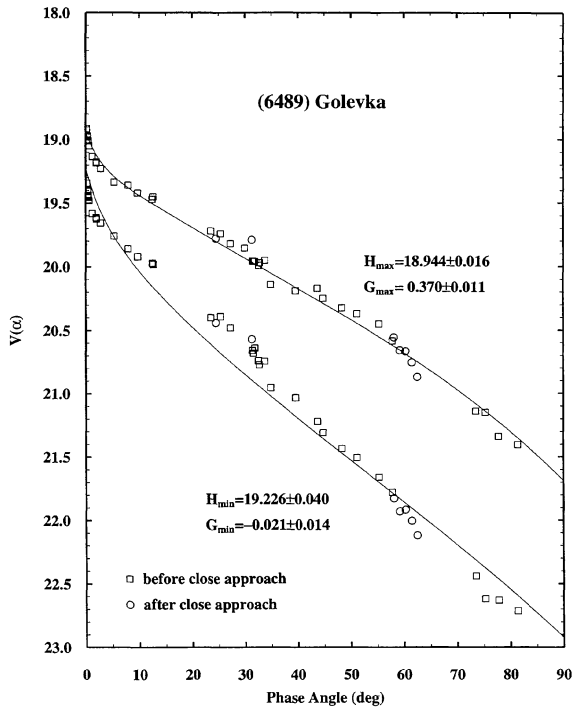

FIG. 5. Phase curves of 6489 Golevka for both the lightcurve maxima and minima. Different symbols represent data acquired before and after the closest approach.

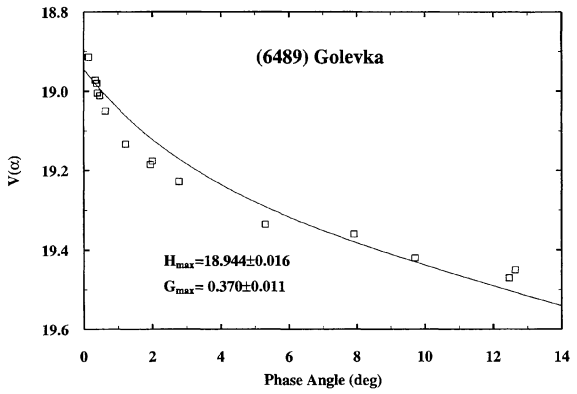

FIG. 6. Low-phase angle region of Fig. 5 for the light curve maxima showing the opposition "spike."

5. MAGNITUDE-PHASE DEPENDENCE

A close approach of an asteroid to the Earth affords the opportunity to make observations at large solar phase angles. In the case of 6489 Golevka we were able to follow the asteroid up to $\alpha=81.4°$, whereas for a typical main-belt object the maximum observable phase angle is around 25°. A particularly favorable encounter geometry also gave us the rare opportunity to perform observations at very small phase angles, enabling us to have a good sampling of the opposition effect region.

Because the brightness of an asteroid depends both on the phase angle and on the aspect angle (and to a lesser degree on the photometric obliquity), we have reduced the observations to a reference geometry—i.e., equatorial aspect—by using the adopted ellipsoidal model derived in the previous section and applying the technique described in Magnusson (1986). Furthermore, the measurements in the *R* band have been used to derive *V* magnitudes by using the *V-R* color index derived in Sec. 3.

Figure 5 shows the phase curves of Golevka for both the lightcurve maxima and minima. Different symbols have been used for data taken before and after the closest approach. Observations performed at similar phase angles but different aspect angles are in good agreement, which indirectly demonstrates the correctness of the applied correction for the reduction to equatorial aspect. The solid lines represent fits of the data points to the *H-G* magnitude system (Bowell *et al.* 1989).

For the lightcurve maxima we obtain $H_{max}=18.944\pm0.016$ and $G_{max}=0.370\pm0.016$, while for the lightcurve minima we obtain $H_{min}=19.226\pm0.040$ and $G_{min}=-0.021\pm0.014$. From the values of the zero-order Fourier coefficients of the individual lightcurves we have also derived mean values for $H=19.074\pm0.029$ and $G=0.138\pm0.013$.

The two-parameter *H-G* magnitude system represents in a reasonably accurate way the behavior of the phase curve for the light curve maxima, including the general slope and the turnover around 45° phase angle. This is less true for the lightcurve minima for which a more irregular trend is apparent. The model also fails to reproduce the abrupt increase in brightness observed at very small phase angles. As shown in Fig. 6, which is an enlargement of the small phase region of Fig. 5, the model appears to systematically overestimate the brightness of the asteroid in the approximate range $0.5°\leqslant\alpha\leqslant7°$, while underestimating the 0° phase brightness by at least 0.1 mag.

This opposition "spike," which amounts to about 0.30 mag/deg at $\alpha\approx0.5°$, has been observed in a few asteroids for which sub-degree phase measurements have been performed—e.g., 44 Nysa (Harris *et al.* 1989)—and seems to be characteristic of high albedo objects. This phenomenon has been interpreted in terms of coherent backscattering (see Muinonen 1994 for a thorough review on the subject).

The large difference between G_{max} and G_{min} implies a strong amplitude-phase angle dependence. By using the same formalism as in Zappalà *et al.* (1990), we have plotted the lightcurve amplitude normalized at zero phase angle versus the solar phase angle (see Fig. 7). A linear regression of the data points gives a normalized slope $m=0.034\pm0.002$ deg^{-1}, a value that is at the upper end of the range which Zappalà *et al.* find for asteroids in their sample. A likely explanation for such a large amplitude-phase relation is the effect of large-scale shadowing on an irregular body (see also Drummond *et al.* 1988, 1991). Specifically, when an object is observed at increasingly large phase angles, topographic reliefs tend to cast large shadows, therefore increasing the steepness of the phase curve. One can expect that such an effect influences light curve minima to a larger extent than lightcurve maxima, because a given relief will in general cast a larger shadow if the local radius of curvature

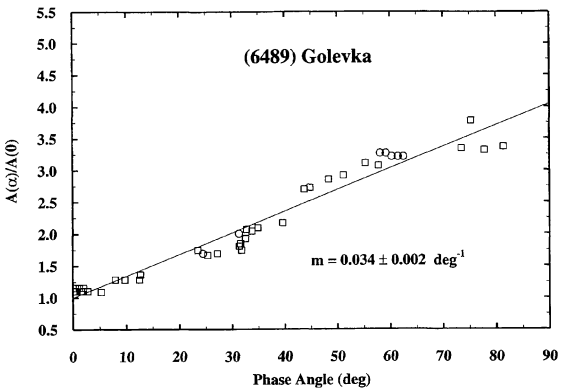

FIG. 7. Amplitude-phase relationship of 6489 Golevka. A linear fit to the data points is also plotted.

of the body is smaller. The net effect should therefore result in a strong amplitude-phase relation for bodies with large-scale topographic structures.

The derived large G_{max} value is typical for very bright asteroids (E, R, or V types; Bowell *et al.* 1989), and seems to confirm a possible V-class membership for this object, as proposed by Hicks & Grundy (1995). On the other hand, the object shows a mean G value which is more characteristic of moderately bright to dark asteroids. This apparent contradiction indicates that other mechanisms (i.e., shadowing) in addition to the regolith photometric properties, are responsible for the behavior of the phase curve.

6. PHOTOMETRIC MODEL

By applying a photometric model to disk-integrated solar phase curves it is in principle possible to describe the scattering properties of a body's surface in terms of model parameters. In this section, we use Hapke's photometric function (Hapke 1981, 1984, 1986), which introduces the following parameters: $\bar{\omega}_0$ (single-scattering albedo), h (opposition surge width), B_0 (opposition surge amplitude), g (single-particle phase function parameter), and $\bar{\vartheta}$ (average slope of macroscopic roughness). The single-particle phase function used in this analysis is a single-term Henyey-Greenstein function, with g defined positive for forward-scattering particles.

The difficulty of applying Hapke's model to ground-based disk-integrated photometry stems from the fact that different sets of model parameters may fit the observations equally well, if data are obtained only over a limited phase angle range as is normally the case for main-belt asteroids (see, e.g., Domingue & Hapke 1989). Furthermore, the opposition effect parameters (B_0 and h) are constrained only by observations at very small phase angles ($0° \leq \alpha \leq 2°$) which are very difficult to obtain. In the course of the Golevka apparition, however, we were able to obtain photometric data spanning phase angles $0.14° \leq \alpha \leq 81.4°$ and were therefore encouraged to model the surface scattering properties of the body in terms of Hapke's theory.

To remove the effect of changing aspect angle from the photometry, the phase curves have been reduced to equatorial aspect, as explained in the previous section. The correct application of the photometric model requires that the angle of incidence and the angle of emergence be computed over the body surface, which in turn requires a detailed knowledge of the asteroid's shape. To overcome this difficulty, we have removed the effects of the rotation lightcurve by using the mean phase curve and computed the photometric function over a sphere. In fact, numerical modeling by Helfenstein & Veverka (1989) has shown that computed phase curves for spheres closely represent the mean phase curves of non-spherical asteroids. The alternative of using an ellipsoidal model, on the other hand, would have introduced two additional parameters (a/b and b/c), thus complicating the task of finding unique solutions, without necessarily providing a better representation of the actual shape.

TABLE 3. Best-fit Hapke parameters for fixed values of $\bar{\vartheta}$.

$\bar{\vartheta}$	g	$\bar{\omega}_0$	h	B_0	χ^2
0°	−0.434	0.557	0.0118	0.772	1.00
5°	−0.434	0.561	0.0118	0.768	1.00
10°	−0.436	0.585	0.0113	0.753	1.00
15°	−0.437	0.623	0.0108	0.739	1.00
20°	−0.444	0.699	0.0095	0.721	1.01
25°	−0.451	0.783	0.0084	0.712	1.04
30°	−0.461	0.873	0.0073	0.712	1.10
35°	−0.473	0.951	0.0064	0.732	1.22

The best-fit values for the parameters have been sought for by integrating numerically the photometric function while varying the input parameters on a five-dimensional grid. As an indicator of the goodness of the fit, the weighted sum of squares of residuals to the mean phase curve (χ^2) has been computed. In order to assess the uniqueness of the solution, we have tabulated the solutions obtained by keeping one parameter fixed at a time, and letting the others vary. In this way it was possible to search for different solutions that produced similarly good fits to the phase curve with different combinations of parameters.

From this procedure, it turned out that the macroscopic roughness parameter was the least constrained by our data set. This fact was expected, because the effects of $\bar{\vartheta}$ on an integral phase curve are mostly visible at phase angles larger than 90° (Helfenstein & Veverka 1989). Table 3 presents the results of the least-squares fitting procedure for the case in which the macroscopic roughness parameter $\bar{\vartheta}$ was kept fixed for each individual run, and forced to assume values from 0° to 35° in 5° steps. The residuals have been normalized to unity for the best solution. It appears from the table that values of $\bar{\vartheta}$ in the range from 0° to 15° produce the best fits to the phase curve. The corresponding residuals, however, differ by less than 1%, and should be considered statistically indistinguishable. On the other hand, solutions corresponding to $\bar{\vartheta}$ values larger than 15° are characterized by increasingly worse fits and unrealistically high values of the single-scattering albedo, and have therefore been rejected. Our best estimate of the Hapke parameters for Golevka can then be derived by averaging the results from Table 3 over the range $0° \leq \bar{\vartheta} \leq 15°$, and taking the scatter of the parameters in this range as a measure of the error. This procedure

results in: $\bar{\vartheta}=7°\pm7°$, $g=-0.435\pm0.001$, $\bar{\omega}_0=0.58\pm0.03$, $h=0.0114\pm0.0004$, $B_0=0.758\pm0.014$. The geometric albedo corresponding to this parameter set is $p_V=0.61\pm0.03$.

The derived parameters are close to the ones computed by Bowell *et al.* (1989) for 44 Nysa, whose phase curve, as noted earlier, exhibits similarities to Golevka's. In particular, both asteroids have a strong backscattering behavior ($g=-0.435$ for Golevka and $g=-0.40$ for Nysa), a high single-scattering albedo ($\bar{\omega}_0=0.58$ for both asteroids) and a comparatively small total opposition effect amplitude ($B_0=0.758$ for Golevka and $B_0=0.6$ for Nysa). Furthermore, both objects display a small opposition effect width parameter ($h=0.0114$ and $h=0.0055$ for Golevka and Nysa, respectively), which is a consequence of the sharp opposition spike observed for both objects.

The geometric albedo implied by the derived parameters is at the upper limit of the range observed for asteroids, making Golevka one of the most reflective minor planets ever observed. However, it might be misleading to directly compare published values of the geometric albedo with values derived from our analysis, because for the vast majority of the objects the reported values are obtained by extrapolation of data taken at phase angles greater than a few degrees, and would therefore underestimate the effect of an opposition spike.

It must be stressed that the errors quoted here for the Hapke parameters do not include any consideration of systematic effects introduced by the violation of the assumptions made, and could therefore be underestimations. In particular, the effects introduced by the irregular shape of the body are difficult to predict. On the positive side, we can say that this close encounter gave us the possibility to apply the current ground-based techniques to determine the scattering properties of an asteroid's surface; should a detailed shape model for Golevka become available as a result of the international radar campaign, it will be possible to test the reliability of our techniques.

7. RADIOMETRIC CONSTRAINTS ON p_V AND D

Thermal infrared observations of 6489 Golevka were made on 1995 June 16 with the CGS3 spectrometer of the UK Infrared Telescope on Mauna Kea through the UKIRT service observing program (Harris *et al.* 1995). The *N*-band magnitude was $m_N=5.98\pm0.52$, based on comparison with the calibration star BS8775. This result implies a 10.6 μm flux of 161 ± 76 mJy at the time of the observations.

Given the absolute magnitude from optical observations, and an appropriate thermal model, the 10.6 μm flux can be used to constrain the size and geometric albedo of the object.

The most commonly used asteroid thermal model is the Standard Thermal Model (STM). This model, described by Lebofsky *et al.* (1986), was used to generate the albedos and diameters published in the *IRAS* Minor Planet Survey (Tedesco ed. 1992). However, a major assumption in this model is that the object is a slow rotator, or has a low thermal inertia, so that thermal emission from the night side can be ignored. While the STM appears to apply well to main-belt asteroids, its applicability to small near-Earth objects is questionable (e.g., Veeder *et al.* 1989). Furthermore, in the case of the Golevka infrared observations the STM is especially inappropriate, due to the large solar phase angle of ~90°. With this geometry, substantial heating and radiation is taking place on the far side of the asteroid. Unfortunately, empirical corrections which are in general applied to account for this effect are not reliable at very large phase angles.

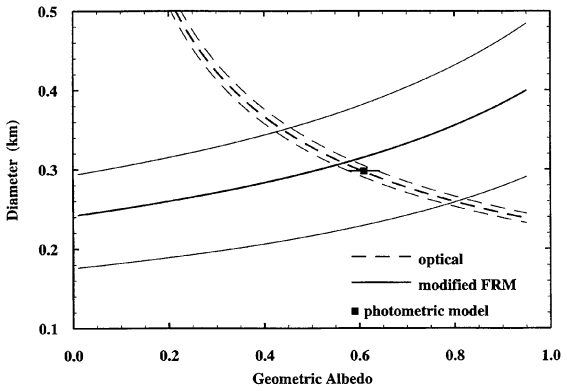

FIG. 8. Diameter vs geometric albedo relations derived from the modified Fast Rotating Model for a 10.6 μm flux of 161 ± 76 mJy (solid curves) and $H=18.82\pm0.05$ (dashed curves). In both cases the lighter curves reflect the uncertainty ranges. A value of 0.9 is assumed for the emissivity. The Fast Rotating Model was modified to take account of the geometry applicable at the time of the infrared observations (see text). The albedo-diameter solution given by the point of intersection of the bold solid and dashed curves is $p_v\sim0.58$ and $D\sim0.3$ km. The photometric model albedo solution ($p_v=0.61\pm0.03$) is also shown.

An alternative is the Fast Rotating Model (FRM) in which it is assumed that the temperature distribution depends only on latitude, i.e., there is no diurnal temperature variation. The FRM applies if the object is a rapid rotator and/or has a high thermal inertia. Albedos are generally lower and diameters higher when derived using the FRM as compared to results from the STM. Since in the FRM half of the thermal emission originates on the night side of the object, a correction for solar phase is not required.

The FRM, in their standard implementations, assume the axis of rotation is perpendicular to the plane containing the line of sight and the Sun. However, in the case of Golevka it is known that the latitude of the sub-Earth point at the time of the infrared observations was about −80°, while the sub-Solar latitude was almost equatorial. For this reason, non-standard versions of the STM and FRM were considered that take account directly of this geometry in the computation of the temperature distribution on the asteroid surface and its thermal emission as seen from the Earth. These two models predict very similar 10.6 μm fluxes, implying that the results are quite insensitive to the asteroid's rotation rate or thermal inertia with the above geometry.

The diameter versus geometric albedo relation implied by the modified FRM, corresponding to a 10.6 μm flux of 161 mJy, is shown as the bold solid curve in Fig. 8 (the lighter solid curves correspond to the error envelope on the 10.6 μm flux). The independent optical diameter/albedo relation (Bowell *et al.* 1989) given by:

$$\log p_V=6.259-2\log D-0.4H,$$

where D is the spherical equivalent diameter in km, is also plotted for $H=18.82\pm0.05$ (dashed curves). The latter quantity is the H-value derived from our optical observations, reduced to $-80°$ sub-Earth latitude and including the opposition spike, and has been chosen for consistency with the viewing geometry described above. The point of intersection of the bold solid and dashed curves gives the best estimate for the albedo-diameter solution, i.e., $D\sim0.30$ km (which for the derived $a/b=1.4$ corresponds to $a\sim0.35$ km; $b\sim0.25$ km) and $p_V\sim0.57$. This result is in good agreement with the independent result ($p_V=0.61\pm0.03$) derived from the photometric model described in Sec. 6.

8. CONCLUSIONS

We have been able to exploit the favorable close approach of 6489 Golevka in 1995 and determine its rotational parameters during a single apparition. The lightcurves reveal an irregular shape, with no significant global color variations across its surface, in the observed spectral bands. The analysis of the integral phase curve in terms of the Hapke photometric theory indicates a body whose surface is characterized by highly reflective and backscattering particles, confirms the presence of a sharp opposition effect at very small phase angles, and suggests a relatively smooth surface at macroscopic scales.

Our measurements indicate that 6489 Golevka is presently in a principal-axis rotational state. Harris (1994) has derived an approximate estimate of the damping time scale of an asteroid in complex rotation to a state of principal axis rotation. For a half-km sized object with a rotation period of 6 hr, Harris' formula gives a damping time of about 500 Myrs. Taken at face value, this result would imply that Golevka has not experienced a major collision event for at least a half billion years.

The application of a modified Fast Rotating Model to thermal infrared measurements in the 10.6 μm band, and the results from the photometric model indicate, despite their uncertainties, that 6489 Golevka is a very small and highly reflective object.

Work at JPL was supported under contract from NASA (A.W. Harris), and by a post-doctoral fellowship from the U.S. National Research Council (W. D. Sears). D. J. Tholen and R. J. Whiteley were supported by NASA Grant NAGW-3044. P. Magnusson was supported by the Swedish National Space Board and by the Swedish Natural Science Research Council. The work of J. Piironen was partly supported by the NorFA foundation, Oslo, Norway. T. Kwiatkowski was supported by the Polish KBN grant 2 P03D 005 09. M. Wolf and P. Pravec were supported by the Grant Agency of the Czech Republic with the grant No. 205-95-1498. The Kharkiv group was supported by the Russian Fund of Fundamental Exploration and by the joint ISF and Ukrainian government Grant U9F200.

REFERENCES

Bowell, E., Hapke, B., Domingue, D., Lumme, K., Peltoniemi, J., & Harris, A. W. 1989, in Asteroids II, edited by R. Binzel, T. Gehrels, and M. Matthews (University of Arizona, Tucson), pp. 524–556
Domingue, D., & Hapke, B. 1989, Icarus, 78, 330
Drummond, J. D., Weidenschilling, S. J., Chapman, C. R., & Davis, D. R. 1988, Icarus, 76, 19
Drummond, J. D., Weidenschilling, S. J., Chapman, C. R., & Davis, D. R. 1991, Icarus, 89, 44
Erikson A., & Magnusson, P. 1993, Icarus, 103, 62
Hapke, B. W. 1981, JGR, 86, 3039
Hapke, B. W. 1984, Icarus, 59, 41
Hapke, B. W. 1986, Icarus, 67, 264
Harris, A. W., Hahn, G., & Davies, J. K. 1995, IAUC, 6181 (June 29)
Harris, A. W. 1994, Icarus, 107, 209
Harris, A. W., & Lupishko, D. F. 1989, in Asteroids II, edited by R. Binzel, T. Gehrels, and M. Matthews (University of Arizona, Tucson), pp. 39–53
Harris, A. W., Young, J. W., Contreiras, L., Dockweiler, T., Belkora, L., Salo, H., & Harris, W. D. 1989, Icarus, 81, 365
Helfenstein, P., & Veverka, J. 1989, in Asteroids II, edited by R. Binzel, T. Gehrels, M. Matthews (University of Arizona, Tucson), pp. 557–593
Helin, E. F. 1991, IAUC, 5268 (May 15)
Hicks, M. D., & Grundy, W. M. 1995, IAUC, 6177 (June 8)
Hudson, R. S., & Ostro, S. J. 1995, BAAS, 27, 1062
Kwiatkowski, T. 1995, A&A, 294, 274
Lagerkvist, C.-I., Barucci, M. A., Capria, M. T., Fulchignoni, M., Guerriero, L., Perozzi, E., & Zappalà, V. 1987, Asteroid Photometric Catalogue (Consiglio Nazionale delle Ricerche, Rome, Italy)
Lebofsky, L. A., *et al.* 1986, Icarus, 68, 239
Magnusson, P. 1986, Icarus, 68, 1
Magnusson, P. 1990, Icarus, 85, 229
Magnusson P., *et al.* 1996, Icarus, 123, 227
Muinonen, K. 1994, in Asteroids, Comets, Meteors 1993, edited by A. Milani, M. Di Martino, and A. Cellino (Kluwer, Dordrecht), pp. 271–296
Ostro, S. J., *et al.* 1991, BAAS, 23, 1144
Ostro, S. J., *et al.* 1995a, BAAS, 27, 1063
Ostro, S. J., *et al.* 1995b, Science, 270, 80
Ostro, S. J., *et al.* 1996, Icarus, 121, 46
Shoemaker, E. M., Williams, J. G., Helin, E. F., & Wolfe, R. F. 1979, in Asteroids, edited by T. Gehrels (University of Arizona, Tucson), pp. 253–282
Spencer, J. R., *et al.* 1995, Icarus, 117, 71
Tedesco, E. F. (ed.) 1992, The IRAS Minor Planet Survey. Phillips Laboratory report PL-TR-92-2049, Hanscom AF Base, MA 01731-3010
Veeder, G. J., Hanner, M. S., Matson, D. L., Tedesco, E. F., Lebofsky, L. A., & Tokunaga, A. T. 1989, AJ, 97, 1211
Williams, G. V. 1995, Minor Planet Circular No. 25418 (July 12)
Zappalà, V., Cellino, A., Barucci, A. M., Fulchignoni, M., & Lupishko D. F. 1990, A&A, 231, 548